"Bent Bonds" between Bismuth and Carbon Atoms as a Result of C–H Activation in Mo–Bi Complexes

Stefan Roggan,[a] Gregor Schnakenburg,[a] Christian Limberg,*[a] Steffen Sandhöfner,[b] Hans Pritzkow,[b] and Burkhard Ziemer[a]

Dedicated to Professor Hubert Schmidbaur on occasion of his 70th birthday

Abstract: The reaction of molybdocenedihydride with two equivalents of $[Bi(OtBu)_3]$ proceeds via alcohol elimination and provides the compound $[Cp_2Mo\{Bi(OtBu)_2\}_2]$ (**1**), which contains two Mo–Bi metal bonds, in good yields. If the two reagents are employed in a 1:1 ratio continuative condensation reactions occur. These initially lead to $[\{Cp_2Mo\}_2\{\mu\text{-}Bi(OtBu)\}_2]$ (**2**), which, however, is very unstable in solution and decomposes via additional alcohol elimination: Complex-induced proximity effects facilitate the cleavage of C–H bonds within the cyclopentadienyl ligands by the residual alkoxide ligands, so that spontaneously two further equivalents of alcohol are released, thereby yielding two isomeric compounds **3** and **4** with Cp ligands bridging Mo–Bi metal bonds: The first isomer (**3**) contains two $\mu_2\text{-}\eta^5\text{:}\eta^1\text{-}C_5H_4$ ligands, the second isomer (**4**) contains one bridging $\mu_3\text{-}\eta^5\text{:}\eta^1\text{:}\eta^1\text{-}C_5H_3$ ligand. The binding of these ligands to molybdenum and bismuth atoms at the same time is made possible through "bent bonds" between the bismuth and certain carbon centres. These unusual bonding situations were analysed by means of calculations based on density functional theory (DFT), the atoms in molecules (AIM) theory, natural bond order (NBO) considerations and the electron localisation function (ELF). According to the results the bonds can be understood in terms of carbanionic centres interacting with bismuth cations (i.e. closed-shell interactions). The formation of these bonds and the thermodynamics/kinetics involved on going from **2** to **3** and **4** were also studied by theoretical methods, so that the product formation is rationalised. The crystal structures of all four new compounds were determined. These structures but also the properties and mechanisms of formation are discussed against the background of the corresponding results obtained while studying the system $[^{Me}Cp_2MoH_2]$/$[Bi(OtBu)_3]$.

Keywords: alkoxides · bismuth · density functional calculations · metalation · molybdenum

Introduction

Recently we have communicated[1] the results of an investigation concerning the reaction between $[^{Me}Cp_2MoH_2]$ and $[Bi(OtBu)_3]$: Three novel complexes (**II**, **III**, **IV**) were identified in course of the reactions shown in Scheme 1. C–H activation reactions initiated by complex-induced proximity effects in **II** allow the formation of **IV** (and also an isomer **IV′** differing from **IV** in the position of the methyl group at the bridging Cp ring), which features a hitherto unprecedented bonding situation, in which a planar $\mu_3\text{-}\eta^5\text{:}\eta^1\text{:}\eta^1\text{-}^{Me}Cp$ ligand bridges three metal centres that are additionally linked through metal–metal bonds. This unusual arrangement is made possible through nonlinear orbital overlaps, that is, "bent bonds" between Bi and C atoms.[1]

Parallel to the investigation outlined above we have studied the parent system with unsubstituted cyclopentadienyl rings, that is, $[Cp_2MoH_2]$/$[Bi(OtBu)_3]$. Surprisingly, this study proved to be notably more demanding, both with regard to synthetic and analytical aspects: It turned out, that changing from the methylcyclopentadienide to the parent cyclopentadienide ligand has a significant chemical influence on the system, for example, on 1) the courses of some of the

[a] S. Roggan, G. Schnakenburg, Prof. Dr. C. Limberg, Dr. B. Ziemer
Humboldt-Universität zu Berlin, Institut für Chemie
Brook-Taylor-Strasse 2, 12489 Berlin (Germany)
E-mail: christian.limberg@chemie.hu-berlin.de

[b] Dr. S. Sandhöfner, Dr. H. Pritzkow
Universität Heidelberg
Anorganisch-Chemisches Institut, Im Neuenheimer Feld 270
69120 Heidelberg (Germany)

Supporting information for this article is available on the WWW under http://www.chemeurj.org/ or from the author.

 DOI: 10.1002/chem.200400836

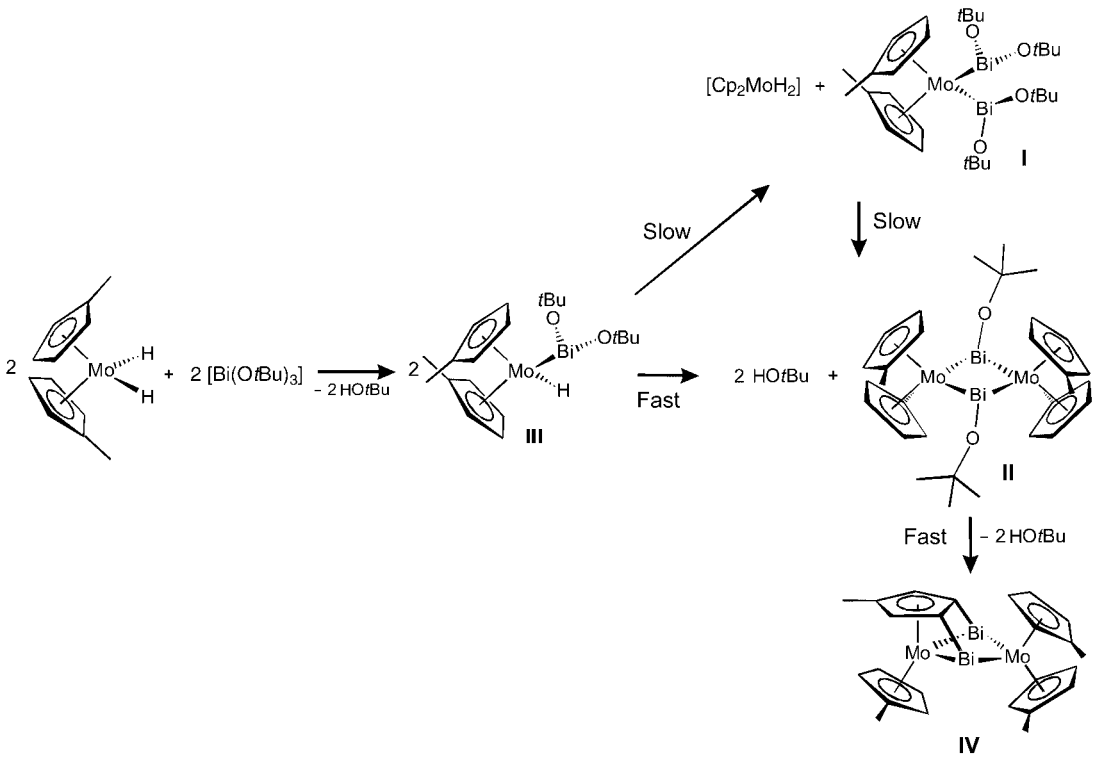

Scheme 1. Products **I**–**IV** of the reaction between [$^{Me}Cp_2MoH_2$] and [Bi(O*t*Bu)$_3$].

reactions, 2) the properties of the compounds, and 3) in one case also on the product formation. Here we report these results in combination with a detailed theoretical analysis of the bonding situations within the products obtained after C–H activation.

Results and Discussion

Formation, investigation and properties of 1–4: The 1:2 reaction of [Cp_2MoH_2] with [Bi(O*t*Bu)$_3$] in toluene provides after workup a bright red solid, which is very sensitive to air and which can be identified as [$Cp_2Mo\{Bi(OtBu)_2\}_2$] (**1**) by NMR spectroscopy (Scheme 2).[2] To obtain structural information about **1**, crystals were grown at −30 °C from hexane and investigated by a single-crystal X-ray diffraction study.

The molecular structure of **1** is depicted in Figure 1. In contrast to the structure of **I**, which contains a crystallographic C_2 axis, the structure of **1** is asymmetric with two different Mo–Bi bond lengths (Mo–Bi1 2.897(2) and Mo–Bi2 2.851(1) Å). Both are comparable to those found in the known MoBi compounds,[2–5] one of them being almost identical to the corresponding bond lengths found in **I** (2.8551(9) Å).[1] As in **I** the Bi–Bi distance (3.526(2) Å; 3.487(2) Å in **I**)) is too long to be interpreted in terms of a Bi–Bi bond, but considering the Bi-Mo-Bi angle of only 75.66(4)° there cannot be significant repulsive forces between the two Bi(OR)$_2$ moieties, either. All other structural data are quite similar in comparison to those of **I**; thus at this stage it appeared that employing [Cp_2MoH_2] (→ **1**) instead of [$^{Me}Cp_2MoH_2$] (→ **I**) did not seem to lead to significant alterations in the reaction.

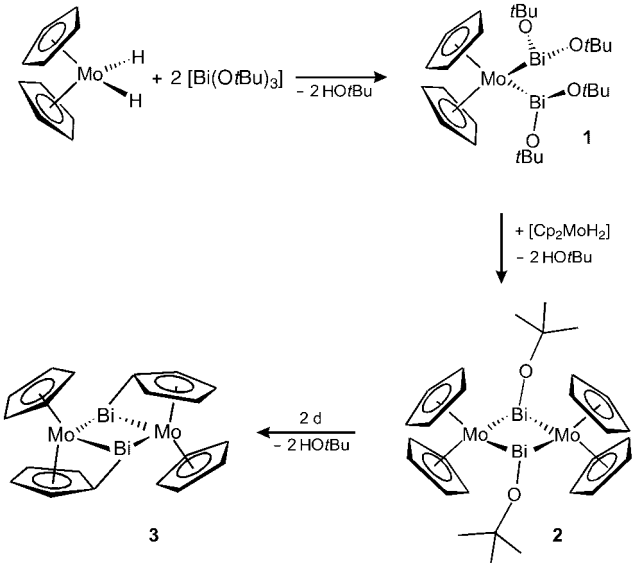

Scheme 2. Products **1**–**3** of the reaction between [Cp_2MoH_2] and [Bi(O*t*Bu)$_3$].

Considering the unstrained nature of **1** it appeared ideally suited for continuative condensation reactions with molybdocene dihydride under elimination of two further equivalents of *tert*-butyl alcohol and the formation of **2** (Scheme 2); hence, the stoichiometry of the two reagents [Cp_2MoH_2] and [Bi(O*t*Bu)$_3$] in Scheme 2 was adjusted from

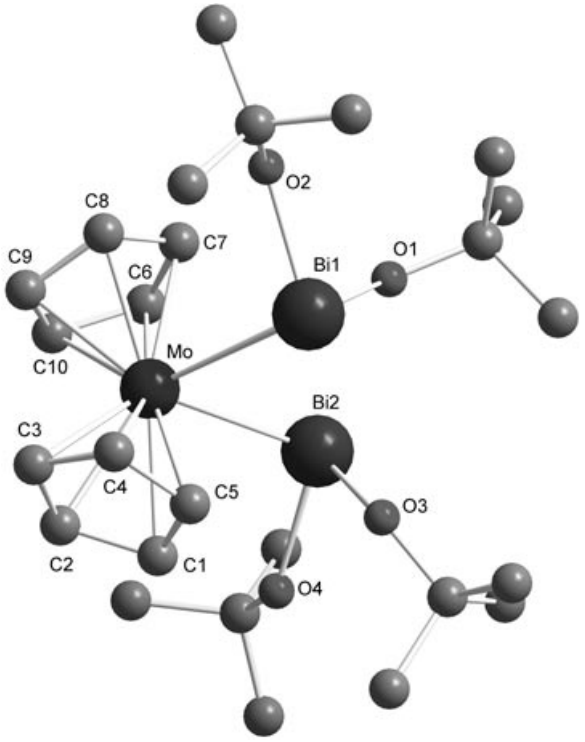

Figure 1. Molecular structure of **1**; all hydrogen atoms were omitted for clarity. Selected bond lengths [Å] and angles [°]: Mo–Bi1 2.897(2), Mo–Bi2 2.851(2), Bi1–O1 2.094(9), Bi1–O2 2.144(8), Bi2–O3 2.151(9), Bi2–O4 2.15(2), Bi1–Bi2 3.526(2); Bi1-Mo-Bi2 75.66(4), O1-Bi1-O2 88.1(3), O3-Bi2-O4 90.0(3), Mo-Bi1-O1 94.1(3), Mo-Bi1-O2 102.8(3), Mo-Bi2-O3 93.5(2), Mo-Bi2-O4 100.6(2).

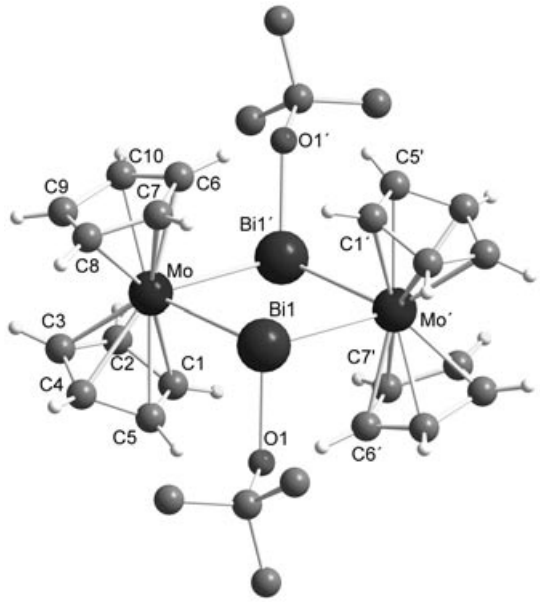

Figure 2. Molecular structure of **2**; the butyl hydrogen atoms were omitted for clarity. Selected bond lengths [Å] and angles [°]: Mo–Bi1 2.916(2), Mo–Bi1′ 2.966(2), Bi1–Bi1′ 3.678(2), Bi1–O1 2.195(8); Bi1-Mo-Bi1′ 77.41(3), Mo-Bi1-Mo′ 102.59(3), Mo-Bi1-O1 102.4(2), Mo′-Bi1-O1 106.2(2).

1:2 (as required for the formation of **1**) to 1:1. Since the methylated analogue of **2**, **II**, is unstable in solution (e.g. in benzene), where it quickly decomposes to give **III**, the isolation of **II** had only been possible after its synthesis in light petrol, from which it precipitates directly after its formation;[1] in the solid state it then appeared reasonably stable at room temperature. Compound **2** proved to be even more reactive: Performing an analogous reaction between $[Cp_2MoH_2]$ and $[Bi(O\mathit{t}Bu)_3]$ in light petrol indeed leads within 6 h to the precipitation of black crystals, whose elemental analysis and spectroscopic data, however, proved that not a single compound but rather two compounds—**2** and its elimination product, that until identification (vide infra) is designated **2**–2*t*BuOH—had crystallised. This means that the rather short time **2** requires for precipitation from petrol is still not short enough to suppress alcohol elimination. Both compounds are insoluble in common organic solvents (note that all compounds depicted in Scheme 1 show good solubilities in benzene!), so that neither a separation by washing nor a spectroscopic characterisation in solution was procurable. However, it proved possible to sort out crystals of **2** mechanically under the microscope so that an X-ray diffraction analysis could be performed, and the crystal structure of **2** is depicted in Figure 2.

The molecule has C_{2h} symmetry with an inversion centre in the middle of the planar Mo_2Bi_2 ring. The Mo–Bi bonds (2.966(2) and 2.916(2) Å) are somewhat longer than those in **1** (2.851(1) and 2.896(1) Å), and the same is true for the Bi–O bonds. Bi-Mo-Bi and Mo-Bi-Mo angles of 77.41(3)° and 102.59(3)°, respectively, are indicative of an unstrained structure (vide supra). The "ligands" around each Bi centre form a distorted tetrahedron (if the imaginary lone pair is considered as a ligand, too) with angles between 102.4(2) and 106.2(2)°. All bond lengths and angles compare well to those of **II**. Particular consideration of the calculated hydrogen positions reveals that some cyclopentadienyl protons are located very closely to the alkoxidic O atoms: For each O atom there are two H atoms, namely those at C6/C5′ and C6′/C5, whose positions are calculated at distances of only 2.230 and 2.217 Å away from it (the corresponding O···C distances are 3.040 and 2.899 Å), and in fact the oxidic free electron pairs can be deduced to point towards these H atoms.

Although the geometrical arrangement of **2** as shown in Figure 2 will be less rigid in solution, the crystal structure indicates the possibility that these or (after rotation) other hydrogen atoms of the Cp rings are situated in very close proximity to the O atoms. This in turn could mean that due to its structure **2** is positioned quite high on the C–H activation barrier already, higher than a Cp ligand and an alkoxidic unit would be when they approach each other from a longer distance (note that for instance **1** does not eliminate alcohol intramolecularly). To cross the residual barrier then less energy is required than in the "long-distance-scenario", that is, within **2** the C–H bonds are activated by complex-induced proximity effects (see below) and they may well be cleaved in solution during a vibration of the molecule under elimination of alcohol, as observed (see below for a more detailed thermodynamic and kinetic discussion).

Having learned that **2** eliminates *t*BuOH so readily in solution, we were interested in an investigation of the equimolar reaction between $[Cp_2MoH_2]$ and $[Bi(OtBu)_3]$ in *toluene*, as we hoped, that the solubility of **2** in this solvent would at least be somewhat higher than in petrol—in fact high enough to allow its *complete* conversion into its elimination product (**2**–2 *t*BuOH) before any precipitation occurs, thereby allowing the investigation of the pure elimination product. This strategy proved to be successful. Addition of toluene to a solid mixture of $[Cp_2MoH_2]$ and $[Bi(OtBu)_3]$ leads to a black solution from which large black crystals precipitate overnight: An IR spectrum revealed the absence of any *tert*-butoxide ligands. A low-resolution mass spectrum showed a peak at *m*/*z* 868 which corresponds to the core $[Cp_2MoBi_2MoCp_2-2H]^+$, and the corresponding formula $C_{20}H_{18}Mo_2Bi_2$ was confirmed by a high-resolution mass spectrum for the isotope $[C_{20}H_{18}{}^{92}Mo_2Bi_2]$ as well as by matrix-assisted laser desorption ionisation (MALDI) measurements and elemental analyses. Such a composition formally arises, when **2** eliminates two equivalents of *tert*-butyl alcohol, so that it was certain that this pure compound corresponded to the one designated **2**–2 *t*BuOH, that had previously contaminated **2** after its synthesis in petrol. Bearing in mind the findings depicted in Scheme 1 it was expected that **2**–2 *t*BuOH would represent a complex analogous to **IV**. However, a single-crystal X-ray diffraction study revealed a different constitution, **3** (the corresponding molecular structure occurs in two split sites within the crystal packing; see Supporting Information): It turned out, that the alcohol eliminations had occurred within two η^5-C_5H_5Mo–$Bi(OtBu)$ moieties thus leading to η^5:η^1-C_5H_4 ligands that bridge the Mo and Bi centres still being connected through metal–metal bonds in compound **3** (Scheme 2, Figure 3). This unusual type of bonding situation (a M–M′ bond that is supported by a η^5:η^1-C_5H_4 ligand) is without precedent in bismuth chemistry, but it has been observed previously for some dinuclear transition-metal compounds (e.g. for the first time in $[Cp(CO)Mo(\mu\text{-}\eta^5\text{:}\eta^1\text{-}C_5H_5)Mn(CO)_4]$[6]).

As in **2** all four metal atoms lie within a plane, and the Mo–Bi bonds that are part of the η^5:η^1-C_5H_4Mo–$Bi(OtBu)$ moieties are with 2.900(2) Å as expected somewhat shorter than the other ones or those found in **2**. To realise the Bi–C bonding two of the four Cp rings are oriented such that their mean planes come to lie almost parallel to the Mo_2Bi_2 plane (one above and one below this plane). The Bi–C bonds thus resulting are somewhat longer (2.28(2) Å) than those found in **IV** (2.24(2) and 2.26(2) Å, respectively),[1] probably since the "metal" ring has to stay planar in **3**, whereas it can fold in **IV**. The peculiar feature about these bonds is the fact that they are bent considerably (by about 40°) out of the plane defined by the cyclopentadienyl rings. This as well as the observation, that the Cp rings bridging the two metals are only slightly distorted from planarity and retain their aromatic character (as evidenced by C–C bond lengths that compare well with those in the other Cp-rings) strongly indicate "bent bonds" between the Bi and the C atoms.

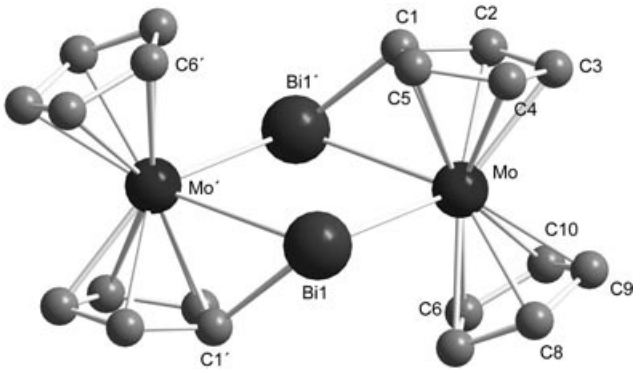

Figure 3. Molecular structure of **3**. Selected bond lengths [Å] and angles [°]: Mo–Bi1 2.922(2), Mo′–Bi1 2.900(2), Bi1′–C1 2.288(9), Bi1–Bi1′ 3.629(2), C1–C2 1.44(2), C2–C3 1.44(2), C3–C4 1.44(2), C4–C5 1.43(2), C5–C1 1.43(2); Bi1-Mo-Bi1′ 77.1(2), Mo-Bi1-Mo′ 102.86(3), Mo-Bi1-C1′ 107.0(2), Mo′-C1′-Bi1 79.1(3), Bi1′-C1-C5 120.1(6).

With a view to gathering some spectroscopic information on **2** or **3** the reaction between $[Cp_2MoH_2]$ and $[Bi(OtBu)_3]$ in the ratio 1:1 was monitored at low temperatures as well as at ambient temperatures by ^{1}H NMR spectroscopy in $[D_8]$toluene. In all those experiments the entire $[Bi(OtBu)_3]$ immediately reacted with half an equivalent of $[Cp_2MoH_2]$ to give (besides the corresponding amounts of *tert*-butyl alcohol) **1**, which accordingly is then present in solution together with $[Cp_2MoH_2]$ in an exact 1:1 ratio. There was no evidence for any monohydride intermediate, as had been observed for the corresponding reaction of $[^{Me}Cp_2MoH_2]$ (compare Scheme 1). This either means that such an intermediate reacts so quickly that it is not detected, or that it is not formed at all. We believe that the latter is the case, since, if the monohydride *was* formed, it should be expected to react in analogy to **III** rapidly and mainly to give **2**, which should attract attention to it by precipitation. However, formation of a precipitate is observed only after several hours: when the sample is left to stand at room temperature the signals of $[Cp_2MoH_2]$ and **1** decrease continuously within two days in favour of those corresponding to the alcohol, while **3** precipitates. However, at no stage did a detectable concentration of **3** or **2** or any other intermediate build up. In conclusion, the methyl substituents on the Cp rings of molybdocenedihydride have a pronounced effect on 1) the course of its reaction with $[Bi(OtBu)_3]$, 2) the solubilities of the products and 3) on the nature of the products—an observation that had not really been expected in advance (a decrease of the solubilities is commonly observed on going from ^{Me}Cp to Cp,[7] but usually to a smaller extent). Naturally the question arose, why in the case of unmethylated molybdocenedihydride was **3** formed and not an isomer **4** corresponding to **IV**. Of course, it could be argued that the crystalline material obtained from the toluene reaction as

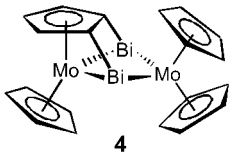

4

described above also contains the isomer **4**, and that by chance a crystal of **3** was picked. Since the solid is insoluble in common organic solvents this hypothesis had to be checked by an X-ray powder diffraction analysis of the bulk crystalline material. The results, however, showed, that the material exclusively contains **3** in the two split sites mentioned above; no signals of a corresponding isomer **4** (see below) were detected.

Nevertheless, finally, we have been able to isolate also the missing analogue of **IV**, **4**: an experiment was performed as described before, the resulting crystals of **3** were isolated by filtration and the filtrate was set aside again. Crystals of **4** precipitated, which were suitable for a single-crystal X-ray structure analysis (Figure 4). Whereas there were no striking features in the crystal structure of **IV**,[1] **4** (like **3**) occurs in two split sites within the crystal packing (see Supporting Information). As in the case of **3** it has to be assumed that **4** is formed starting from **2** with the difference that only one Cp ligand is involved in the elimination reaction, that is, the two equivalents of alcohol were eliminated from a η^5-CpMo(Bi(O*t*Bu))$_2$ moiety, so that both Bi centres are connected to the same ring. To check the purity of the second

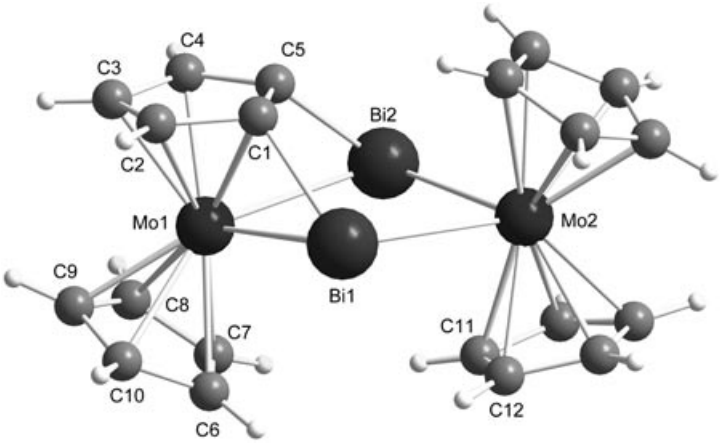

Figure 4. Molecular structure of **4**. Selected bond lengths [Å] and angles [°]: Mo2–Bi1 2.914(2), Mo2–Bi2 2.901(2), Mo1–Bi1 2.914(2), Mo1–Bi2 2.897(2), Bi2–C5 2.25(2), Bi1–C1 2.28(2), Bi1–Bi2 3.530(2), C1–C5 1.45(2), C1–C2 1.43(2), C2–C3 1.43(2), C3–C4 1.46(2), C4–C5 1.46(2); Bi1-Mo1-Bi2 74.76(3), Mo2-Bi1-Mo1 103.83(3), Mo2-Bi1-Mo1 104.56, Mo1-Bi1-C1 49.3(3), Mo2-C5-Bi1 80.3(4), Bi1-C1-C5 117.3(10), C2-C1-C5-C4 –1.2(15), C3-C4-C5-C1 2.6(15).

batch of crystals isolated from the mother liquor, as before a powder diffraction measurement was performed. This revealed the presence of **3** beside **4** (1:1 ratio); the reasons for this somewhat peculiar product formation and crystallisation behaviour are addressed in the theoretical section below. Compound **IV** had been the first precedent for a complex, in which a still almost planar μ_3-η^5:η^1:η^1-Cp ligand bridges three metal centres that are additionally linked by metal–metal bonds, and such an arrangement is observed here, too. All structural data are quite similar to those observed in **IV**, that is, the Mo_2Bi_2 ring is folded along the Bi–Bi axis and the Bi–C bonds are shorter than those in **3**. As in **IV**, all structural parameters for **4** suggest non-linear orbital interactions, that is, "bent bonds" between the Bi and the C atoms.

The analysis of this feature had been initiated in the case of **IV** by preliminary density functional theory (DFT)/Bader calculations at the B3LYP/[Lanl2dz] (Stuttgart RSC 1997, ECP (Mo) cc-pVDZ-PP (Bi)) level of theory.[1] Below the results of the computationally very demanding all-electron treatment of **4** as well as the corresponding investigation of the novel compound **3**, the determination of the electron localisation function (ELF), the detailed analysis of the results and their interpretation are reported.

Theoretical analysis of the "bent" Bi–C bonds and the reaction paths leading to them: Gradient corrected DFT calculations of **3** and **4** were carried out without symmetry restraints by using B3LYP functionals and the Lanl2dz basis set (=basis set "I").[8] The calculated geometrical parameters compare well with the experimental values (cf. Supporting Information). All-electron single-point calculations using the WTBS[9] basis set for Mo and Bi and 6–311G* for H and C (=basis set "II") were done to improve the quality of the wavefunction and exclude pseudo-potential effects. The calculated electronic structures were analysed by various quantum-chemical methods to obtain further information about the bonding situation in these systems. Both isomers **3** and **4** are very close in energy, but isomer **3** lies somewhat higher than **4** (about 9 kJ mol^{-1} (B3LYP/I) and about 12 kJ mol^{-1} (B3LYP/II), respectively).

The non-linear Bi–C interaction in **3** and **4** can be nicely seen in the orbital analysis of the wavefunction. Several Kohn–Sham orbitals contribute significantly to the Bi–C interaction. A Mulliken bonding population analysis reveals an overall overlap population of 0.362 (0.384) between Bi and C in **3** (**4**), an overlap population using extended Hückel theory[10] yields an overlap population of 0.678 (0.691) for **3** (**4**) (cf. Supporting Information). The high Wiberg bond index (WBI) between the bismuth and carbon centres of 0.84 in **3** (0.86 in **4**) indicates a comparatively strong covalent interaction. Natural bond orbital analyses[11] of **3** and **4** show 2c–2e natural bonds that are polarised towards the carbon atoms and consist of an $sp^{2.36}$ ($sp^{1.91}$) hybrid at carbon and a p orbital at the bismuth centre in **3** (**4**) (Table 1). Both natural bond orbitals are displayed in Figure 5.

Table 1. Results of the NBO analyses of **3** and **4** at the B3LYP/II//B3LYP/I level of theory.

	NPA[a] partial charges	NBO analysis[b] occ.	%(Bi)	hyb.	%(C)	hyb.	E_{NBO}	WBI
3	Mo: –0.34 Bi: 0.82 C: –0.44	1.94	24.0	p	76.0	$sp^{2.36}$	–0.369	0.84
4	Mo: –0.32 Bi: 0.80 C: –0.46	1.80	26.2	p	73.8	$sp^{1.91}$	–0.376	0.86

[a] Natural population analysis. [b] Natural bond orbital analysis of the Bi–C bond: NBO occupancy (occ.), bond polarization in %(Bi) and %(C), orbital hybridization (hyb.), energy of the NBO (E_{NBO}) and Wiberg bond index (WBI).

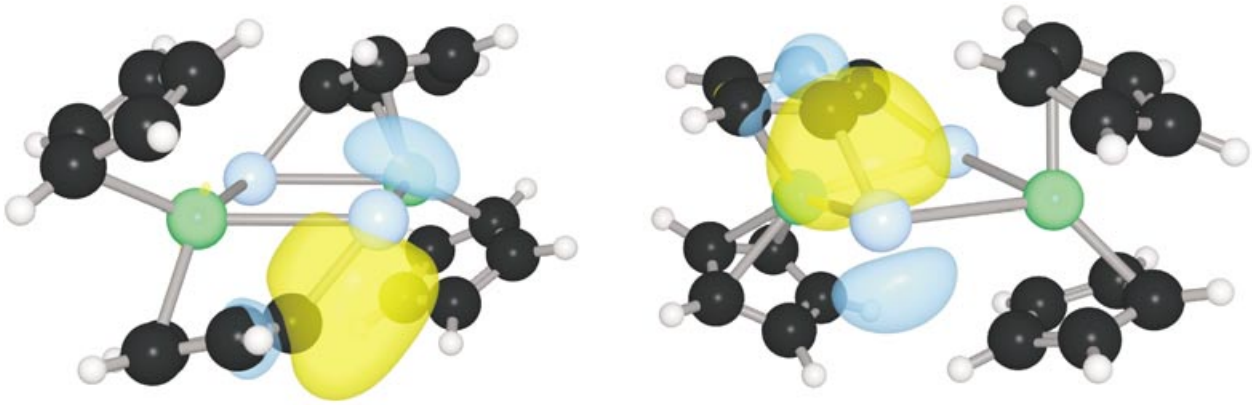

Figure 5. Natural bond orbital of the Bi–C bond in **3** (left) and **4** (right).

The topological analysis of the electron density ρ using the atoms in molecules (AIM) theory[12] pioneered by Bader confirms this situation. The existence of bond critical points between the respective Bi and C atoms argue for Bi–C bonding (Figure 6). The significant ellipticity of the Bi–C bond at the critical point (**3**: 0.18, **4**: 0.18) reflects the curvature of this bond. A comparison of the Hessian (the so-called electron energy density) at the critical points $\mathscr{H}(r_c)$, shows that the Bi–C bonds in both compounds are of comparable strength and covalency (**3**: −0.169, **4**: −0.186 Hartree Å^{-3}). The high values of the Laplacian of the electron density $\bigtriangledown^2\rho(r_c)$ (**3**: 5.65, **4**: 5.79 e Å^{-5}) in combination with

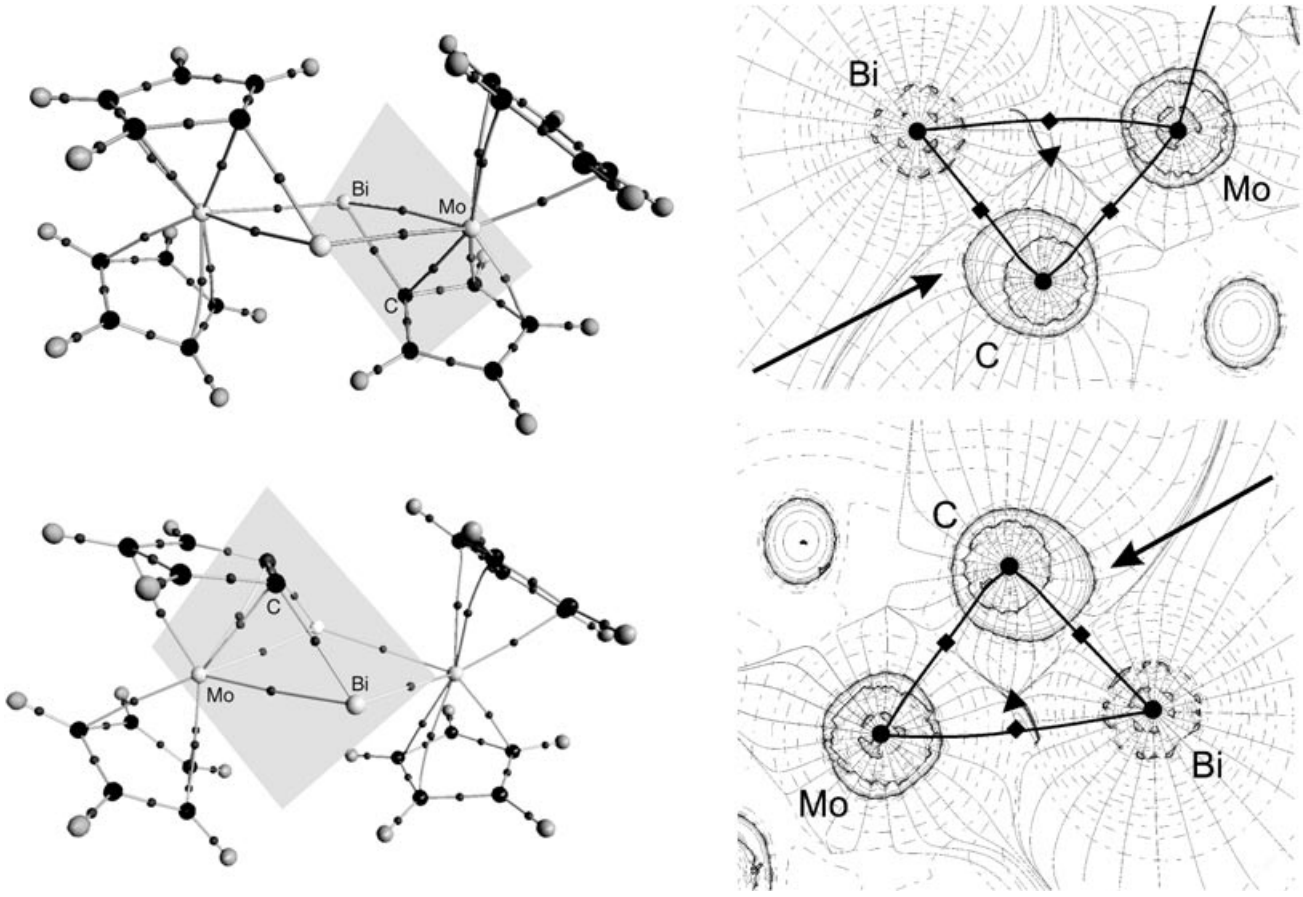

Figure 6. Three-dimensional representations of molecular graphs resulting from AIM analysis of **3** (top left) and **4** (bottom left). Ring and cage critical points are omitted for clarity. The two-dimensional cross section (light grey Mo-C-Bi-plane, right) represents the Laplace distribution with bond critical points (squares), ring critical points (triangles) and nucleus positions (circles). The arrows show electron density concentration aside from the Bi–C atomic interaction lines.

the relatively low electron density $\rho(r_c)$ at the bond critical points (**3**: 0.616, **4**: 0.616 e Å^{-3}) indicate electron depletion and contraction of the charge density towards the nuclei and therefore suggest closed shell (C–Bi) donor/acceptor interactions as already shown by the highly polarised natural bond orbitals. The electron localisation function[13] (ELF) in **3** and **4** shows no local maximum on the Bi–C bonding line, but regions of localized electron density are apparent, which are not symmetric with respect to the two atoms and are strongly shifted away from the bonding lines between the nuclei indicating the bent character of the Bi–C interaction (Figure 7).

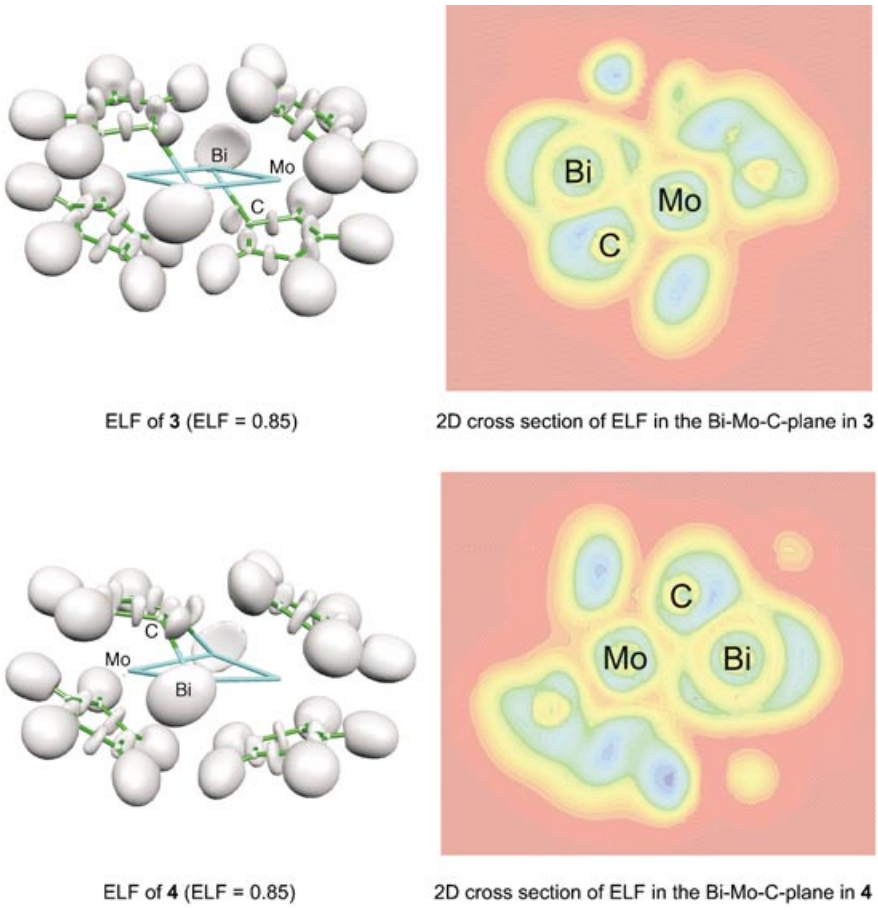

Figure 7. Results obtained utilising the ELF for the analysis of **3** and **4**.

To obtain information about the thermodynamics (is ΔG positive or negative?) and the kinetics (height of the C–H activation barriers) involved in the formation of these bonds, the reaction of **2** to give **3** and **4** was also studied at the BP86/Lanl2dz level of theory using density fitting.[8] It turned out that ΔE for the first alcohol elimination, that is, the first step that is necessary for the formation of both **3** and **4**, is 76.9 kJ mol^{-1}. However, since two molecules are generated from one there is a gain in entropy that leads to a ΔG value of 25.1 kJ mol^{-1} (ΔG values are computed at standard conditions (298.15 K/1 atm)). The reaction is thus only slightly endothermic. $\Delta G^{\neq}$ is 89.2 kJ mol^{-1}, that is, the barrier can be easily crossed at room temperature; in the absence of complex-induced proximity effects it would probably be much higher. The resulting intermediate **A** (Figure 8) is separated by a considerable barrier of 133.0 kJ mol^{-1} from its isomer **B**, which is generated by an edge inversion[21] of the second $[Mo]_2Bi–OtBu$ unit. **A** and **B** basically have the same energy and by eliminating a further equivalent of alcohol they give **3** and **4**, respectively, through moderate barriers (**A** → **3**, **B** → **4**) of comparable height ($\Delta\Delta G^{\neq}$ = 3.2 kJ mol^{-1}). As pointed out above, **3** and **4** differ only slightly in energy, too, but the trend as revealed by B3LYP (9 and 12 kJ mol^{-1}, respectively, in favour of **4**) is confirmed by calculations at the B86 level of theory (11.8 kJ mol^{-1}). Figure 8 summarises all these theoretical results concerning the kinetic and thermodynamic situation in the system which may serve to rationalise the very peculiar observation that the reaction between $[Cp_2MoH_2]$/$[Bi(OtBu)_3]$ first of all leads to pure crystals of **3** in good yields, while on setting aside the mother liquor after separation of the first bunch of crystals a 1:1 mixture of **3** and **4** is isolated.

First of all it is evident that all the reactions should represent equilibria lying on the side of the starting materials. However, the final products are constantly removed from these equilibria through precipitation, so that the reactions are nonetheless driven to the product side.

Starting from **2** intermediate **A** has to form, and a second alcohol elimination starting from **A** necessarily leads to **3**. Hence, **3** enriches the solution first, and as a very low concentration is already sufficient for its precipitation, **3** crystallises selectively during the starting period of the reaction. For the formation of **4**, **A** would have to isomerise into **B** first. However, as the corresponding barrier of 133.0 kJ mol^{-1} is substantially higher than the competitive barrier (83.7 kJ mol^{-1}) leading to **3** (continuously crystallising from solution!) the inversion process is initially not of relevance, that is, **3** is favoured kinetically. After separation of the first batch of crystals from the mother liquor the energetic situation is naturally the same, but considerable amounts of *t*BuOH are now present in solution that accelerate the reverse reactions. Consequently, the alcohol slows

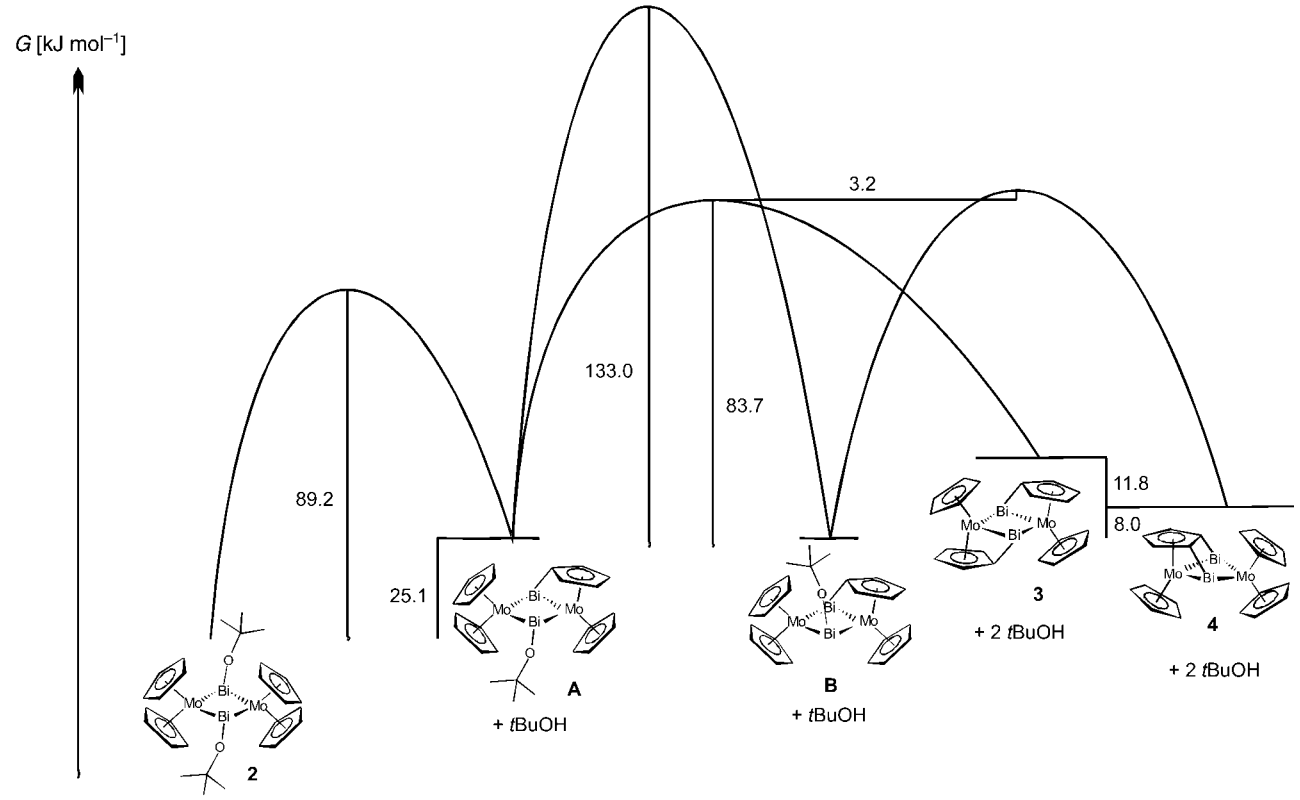

Figure 8. ΔG and $\Delta G^{\neq}$ values for the conversion of **2** to **3** and **4** as obtained with BP86/Lanl2dz using density fitting.

down the precipitation of **3**, so that the concentrations of the species **A** and **B**—and thus also those of **3** and **4**—are determined by thermodynamic arguments, which even slightly favour **4**. Therefore, compounds **3** and **4** crystallise at the same time in an almost 1:1 ratio.

Conclusion

Only recently an intramolecular carbanion attack at a non-acidic C–H bond was reported[14] to occur within a calcium complex, and this process has been discussed against the background of cyclometallation reactions found in early-transition metal chemistry (e.g. the formation of "tuck-in" complexes, Scheme 3)[15] as well as *ortho*-directed lithiations.[16]

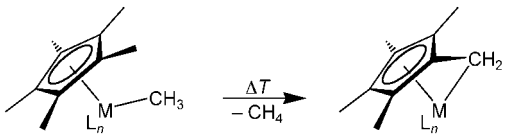

Scheme 3. Formation of "tuck-in" complexes.

Such a comparison is all the more appropriate considering the conversion of **2** to **3** and **4**, since it is clear here that the reacting groups are in fact located very closely to each other, so that complex-induced proximity effects can become effective. Whereas the structure of **2** is ideally pre-arranged for the elimination of two equivalents of alcohol leading to **3**, formation of **4** requires a sequential process: Subsequent to the first Bi–C bond formation the resulting molecule **A** has to rearrange by an edge inversion of the second $[Mo]_2Bi–O$*t*Bu unit, so that both Bi atoms get linked to the same ring. The barrier for this inversion is substantially higher than the one leading from **A** to **3**; thus, **3** is kinetically favoured over **4** and formed selectively in the first period of the reaction. While the reaction proceeds, the concentration of *t*BuOH rises, which finally enables simultaneous formation of thermodynamically favoured **4** by influencing the state of the equilibria involved.

It remains unclear why the reaction of $[^{Me}Cp_2MoH_2]$ yields exclusively the analogue of **4**, **IV**, whereas $[Cp_2MoH_2]$ yields mainly **3**. Considering the results presented here a combination of crystallisation properties and thermodynamics is likely to be responsible. Future research will now focus on the investigation of further electronic/inductive effects on this novel type of C–H activation as well as on the analogous cleavage of other types of C–E bonds.

Experimental Section

All manipulations were carried out in a glove-box, or by means of Schlenk-type techniques involving the use of a dry argon atmosphere.

Solvents were purified, dried and degassed prior to use. Microanalyses were performed by the Analytische Laboratorien des Organisch-Chemischen-Institutes der Universität Heidelberg by using a CHN-Analyser Heraeus. Infrared (IR) spectra were recorded using samples prepared as KBr pellets with a Digilab Excalibur FTS 3000 FTIR-spectrometer. X-ray powder diffraction data were collected with a XRD 7 Seiffert-FPM using $Cu_{K\alpha}$ radiation. Low-resolution mass spectra were recorded on a Finnigan MAT 8400. High-resolution mass spectra were performed by the Zentrum für Massenspektrometrie des Organisch-Chemischen-Instituts der Universität Heidelberg by using a JEOL JMS-700 spectrometer. The ions were generated by EI (70 eV). $[Cp_2MoH_2]$ and $[Bi(OtBu)_3]$ were prepared as described.[7,17,18]

1: Synthesis and spectroscopic data: see reference [2]. Elemental analysis calcd (%) for $C_{26}H_{46}Bi_2MoO_4$: C 33.56, H 5.00; found: C 33.34, H 4.95.

2: A solution of $[Bi(OtBu)_3]$ (0.094 g, 0.22 mmol) in light petrol (2 mL) was added to a suspension of $[Cp_2MoH_2]$ (0.050 g, 0.22 mmol) in light petrol (1 mL). Agitation resulted in a red solution, which was filtered and stored at room temperature. Small amounts of black needles formed overnight, that were suitable for single-crystal X-ray structure analysis. The elemental analysis indicates that **2** is formed only in small amounts, while the bulk consists of **3**.

3 and **4**: Toluene (10 mL) was added to a solid mixture of $[Cp_2MoH_2]$ (0.200 g, 0.88 mmol) and $[Bi(OtBu)_3]$ (0.375 g, 0.88 mmol) at room temperature. A red solution was initially formed that spontaneously turned black after about 120 s. Leaving the solution overnight at room temperature without stirring led to crystalline **3** (0.262 g, 0.26 mmol), which after separation from the solution by decanting, washing repeatedly with light petrol and drying was analytically pure (yield: 59%); according to powder diffraction data these crystals are not contaminated by crystals of the isomer **4**. Elemental analysis calcd (%) for $C_{20}H_{18}Mo_2Bi_2$: C 27.67, H 2.08, found: C 27.77, H 2.17; IR (KBr): $\tilde{\nu}$ = 3078 m, 1630 w, 1406 m, 1310 m, 1169 m, 1096 s, 1059 m, 995 m, 915 m, 829 s, 775 s, 646 m, 593 w, 508 w, 458 m, 417 m cm^{-1}; low-resolution MS (EI): *m*/*z* (%): 870 (40) $[M^+]$, 660 (80) $[M^+-Bi]$, 448 (100) $[M^+-2Bi]$, 209 (45) $[Bi^+]$, 65 (20) $[Cp^+]$; high-resolution $C_{20}H_{18}{}^{92}Mo^{92}MoBi_2$: *m*/*z* 859.9218 (859.9152, Δm = 6.0 mm). When the mother liquor was left to stand for for three days a 1:1 mixture of crystalline **3** and **4** precipitated. There are no marked differences between the spectroscopic data of **3** and **4** so that a distinction was only possible by X-ray powder diffraction.

X-ray crystallography: The data of **1**, **2** and **3** were collected (Table 2) on a Nonius Kappa CCD spectrometer, the data of **4** on a Stoe IPDS I instrument using $Mo_{K\alpha}$ radiation, λ = 0.71073 Å. In all cases, the structures were solved by direct methods (program: SHELXS-97)[19] and refined versus F^2 (program: SHELXL-97)[20] with anisotropic temperature factors for all non-hydrogen atoms. All hydrogen atoms were added geometrically and refined by using a riding model.

CCDC-244338–244341 contain the supplementary crystallographic data for this paper. These data can be obtained free of charge via www.ccdc.cam.ac.uk/conts/retrieving.html (or from the Cambridge Crystallographic Data Centre, 12 Union Road, Cambridge CB2 1EZ, UK (Fax: (+44)1223-336-033; E-mail: deposit@ccdc.cam.ac.uk).

Acknowledgement

We are grateful to the Deutsche Forschungsgemeinschaft, the Fonds der Chemischen Industrie, the BMBF, the Dr. Otto Röhm Gedächtnisstiftung and to the Humboldt-Universität zu Berlin for financial support. We also thank Prof. Gottfried Huttner and Prof. Alexander C. Filippou for helpful discussions, as well as Thoralf Krahl for recording the powder data. G. S. additionally thanks the Graduiertenkolleg 352/3: "Synthetische,

Table 2. Crystallographic data for **1**–**4**.

	1	**2**	**3**	**4**
empirical formula	$C_{26}H_{46}Bi_2MoO_4$	$C_{28}H_{38}Bi_2Mo_2O_2$	$C_{20}H_{18}Bi_2Mo_2$	$C_{20}H_{18}Bi_2Mo_2$
molecular mass	936.53	1016.42	868.2	868.2
crystal size [mm]	0.20×0.20×0.05	0.20×0.20×0.10	0.07×0.10×0.10	0.36×0.24×0.16
crystal system	monoclinic	monoclinic	monoclinic	monoclinic
space group	C_2/c	$P_2(1)/c$	$P_2(1)/n$	C_2/c
Z	8	2	2	8
a [Å]	30.819(6)	10.649(2)	8.222(3)	23.319(4)
b [Å]	10.626(2)	14.483(3)	8.447(3)	7.750(1)
c [Å]	20.616(4)	9.637(2)	13.110(6)	20.951(3)
α [°]	90	90	90	90
β [°]	115.27(3)	111.12(3)	91.468(5)	102.81(3)
γ [°]	90	90	90	90
V [$Å^3$]	6105(2)	1386.4(5)	910.2(6)	3692.1(9)
ρ_{calcd} [$g\,cm^{-3}$]	2.038	2.435	3.175	3.124
T [K]	200(3)	200(3)	103(2)	150(2)
corrns	Lorentz-polarisation-factor			
absorption correction	Semi-empirical from equivalents			
μ [mm^{-1}]	11.932	13.561	20.620	20.333
F(000)	3536	944	780	3104
hkl range	*h:* −39 to 39	*h:* −13 to 13	*h:* −11 to 11	*h*: −28 to 28
	k: −13 to 12	*k:* −16 to 17	*k:* 0 to 11	*k*: −9 to 9
	l: −26 to 26	*L:* −11 to 11	*l:* 0 to 17	*l*: −25 to 25
Θ range [°]	1.46 to 27.50	2.49 to 26.04	3.46 to 30.44	2.78 to 25.49
measured reflections	12762	4211	8835	15453
independent reflections	6923	2580	2521	3426
observed refl. [$I > 2\sigma(I)$]	3763	1814	2300	3074
parameters	312	159	119	211
R_1	0.0723	0.0499	0.0371	0.0489
wR_2	0.1493	0.1051	0.0957	0.1051
R (all)	0.1462	0.0810	0.0449	0.0555
residual el. density [$e\,Å^{-3}$]	+2.506/−2.154	+1.533/−1.514	+2.830/−2.364	+3.356/−2.013

mechanistische und reaktionstechnische Aspekte von Metallkatalysatoren" as well as the HLRN super computing center.

[1] S. Roggan, C. Limberg, B. Ziemer, M. Brandt, *Angew. Chem.* **2004**, *116*, 2906–2910; *Angew. Chem. Int. Ed.* **2004**, *43*, 2846–2849.
[2] M. Hunger, C. Limberg, E. Kaifer, P. Rutsch, *J. Organomet. Chem.* **2002**, *641*, 9.
[3] W. Clegg, N. A. Compton, R. J. Errington, N. C. Norman, A. J. Tucker, M. J. Winter, *J. Chem. Soc. Dalton Trans.* **1988**, 2941.
[4] W. Clegg, N. A. Compton, R. J. Errington, N. C. Norman, *Polyhedron* **1988**, *7*, 2239.
[5] Compare reference [10] in reference [2].
[6] R. Hoxmeier, B. Deubzer, H. D. Kaesz, *J. Am. Chem. Soc.* **1971**, *93*, 536.
[7] L. Lugo, G. Lanza, I. L. Fragala, C. L. Stern, T. J. Marks, *J. Am. Chem. Soc.* **1998**, *120*, 3111.
[8] Calculations were done by using Gaussian03 where the B3LYP functionals and LANL2DZ basis set are implemented. BP86 calculations were done using density fitting with automated calculated auxiliary basis sets. Gaussian 03, Revision B.05, M. J. Frisch, G. W. Trucks, H. B. Schlegel, G. E. Scuseria, M. A. Robb, J. R. Cheeseman, J. A. Montgomery, Jr., T. Vreven, K. N. Kudin, J. C. Burant, J. M. Millam, S. S. Iyengar, J. Tomasi, V. Barone, B. Mennucci, M. Cossi, G. Scalmani, N. Rega, G. A. Petersson, H. Nakatsuji, M. Hada, M. Ehara, K. Toyota, R. Fukuda, J. Hasegawa, M. Ishida, T. Nakajima, Y. Honda, O. Kitao, H. Nakai, M. Klene, X. Li, J. E. Knox, H. P. Hratchian, J. B. Cross, C. Adamo, J. Jaramillo, R. Gomperts, R. E. Stratmann, O. Yazyev, A. J. Austin, R. Cammi, C. Pomelli, J. W. Ochterski, P. Y. Ayala, K. Morokuma, G. A. Voth, P. Salvador, J. J. Dannenberg, V. G. Zakrzewski, S. Dapprich, A. D. Daniels, M. C. Strain, O. Farkas, D. K. Malick, A. D. Rabuck, K. Raghavachari, J. B. Foresman, J. V. Ortiz, Q. Cui, A. G. Baboul, S. Clifford, J. Cioslowski, B. B. Stefanov, G. Liu, A. Liashenko, P. Piskorz, I. Komaromi, R. L. Martin, D. J. Fox, T. Keith, M. A. Al-Laham, C. Y. Peng, A. Nanayakkara, M. Challacombe, P. M. W. Gill, B. Johnson, W. Chen, M. W. Wong, C. Gonzalez, J. A. Pople, Gaussian, Inc., Pittsburgh PA, **2003**.
[9] WTBS basis set: S. Huzinaga, B. Miguel, *Chem. Phys. Lett.* **1990**, *175*, 289 and S. Huzinaga, M. Klobukowski, *Chem. Phys. Lett.* **1993**, *212*, 260. Basis sets were obtained from the Extensible Computational Chemistry Environment Basis Set Database, Version 02/25/04, as developed and distributed by the Molecular Science Computing Facility, Environmental and Molecular Sciences Laboratory which is part of the Pacific Northwest Laboratory, P. O. Box 999, Richland, Washington 99352, USA, and funded by the U. S. Department of Energy. The Pacific Northwest Laboratory is a multi-program laboratory operated by Battelle Memorial Institute for the U. S. Department of Energy under contract DE-AC06–76RLO 1830. Contact David Feller or Karen Schuchardt for further information.
[10] a) C. Mealli, D. M. Proserpio, *MOAN & C. A. C. A. O.* PC Beta Version 5.0, **1998**; b) C. Mealli, D. M. Proserpio, *J. Chem. Educ.* **1990**, *67*, 399.
[11] E. D. Glendening, J. K. Badenhoop, A. E. Reed, J. E. Carpenter, J. A. Bohmann, C. M. Morales, F. Weinhold, *NBO 5.0 Program*, Theoretical Chemistry Institute, University of Wisconsin, Madison, **2001**.
[12] F. Biegler-König, J. Schönbohm, AIM 2.0 2002, Morphy 98. P. L. A. Popelier, R. G. A. Bone, UMIST, Manchester, England, EU 1998.
[13] a) ELF Analysis was performed using the TopMOD suite of programs. S. Noury, X. Krokidis, F. Fuster, B. Silvi, *TopMod package*, Laboratoire de Chimie Théorique, Université Pierre et Marie Curie, Paris, France, **1997**; b) visualisation of ELF was done using MOLEKEL 4.3, P. Flükiger, H. P. Lüthi, S. Portmann, J. Weber, Swiss Center for Scientific Computing, Manno (Switzerland), 2000–2002. Stefan Portmann & Hans Peter Lüthi. MOLEKEL: An Interactive Molecular Graphics Tool. *CHIMIA* **2000**, *54*, 766–770.
[14] S. Harder, *Angew. Chem.* **2003**, *115*, 3553; *Angew. Chem. Int. Ed.* **2003**, *42*, 3430.
[15] Review: I. P. Rothwell, *Polyhedron* **1985**, *4*, 177; compare ref. in reference [14].
[16] W. Bauer, P. von R. Schleyer, *J. Am. Chem. Soc.* **1989**, *111*, 7191.
[17] A. R. Dias, M. L. H. Green, *J. Chem. Soc. D* **1969**, 962; A. R. Dias, M. L. H. Green, *J. Chem. Soc. A* **1971**, 2807.
[18] M. Massiani, R. Papiernik, L. G. Hubert-Pfalzgraf, J. C. Daran, *Polyhedron* **1991**, *10*, 437.
[19] SHELXL-97, G. M. Sheldrick, Program for Crystal Structure Refinement, University of Göttingen, **1997**.
[20] SHELXS-97, G. M. Sheldrick, Program for Crystal Structure Solution, University of Göttingen, **1997**.
[21] A. J. Arduengo, D. A. Dixon, D. C. Roe, *J. Am. Chem. Soc.* **1986**, *108*, 6821.

Received: August 13, 2004
Published online: November 17, 2004